Atmospheric Environment 272 (2022) 118945

Contents lists available at ScienceDirect

Atmospheric Environment

journal homepage: www.elsevier.com/locate/atmosenv

Estimating long-term $PM_{10-2.5}$ concentrations in six US cities using satellite-based aerosol optical depth data

Meredith Pedde [a,*], Itai Kloog [b], Adam Szpiro [c], Michael Dorman [b], Timothy V. Larson [d,e], Sara D. Adar [a]

[a] Department of Epidemiology, University of Michigan School of Public Health, Ann Arbor, MI, USA
[b] Department of Geography and Environmental Development, Ben-Gurion University of the Negev, Beer Sheva, Israel
[c] Department of Biostatistics, University of Washington, Seattle, WA, USA
[d] Department of Environmental and Occupational Health Sciences, University of Washington, Seattle, WA, USA
[e] Department of Civil & Environmental Engineering, University of Washington, Seattle, WA, USA

HIGHLIGHTS

- We predicted $PM_{10-2.5}$ using satellite-based daily AOD data.
- Long-term $PM_{10-2.5}$ predictions correlated well with measurements in 5 study areas.
- Predictions performed better spatially than nearest-monitor and IDW alternatives.

ARTICLE INFO

Keywords:
$PM_{10-2.5}$
Coarse PM
Aerosol optical depth (AOD)
Air pollution
Spatial prediction model
Satellite

ABSTRACT

A major challenge in assessing the health risks of $PM_{10-2.5}$ is the limited ground-level measurement data from which to estimate exposure. This is especially problematic for studying long-term $PM_{10-2.5}$ health effects since $PM_{10-2.5}$ is more spatially variable than $PM_{2.5}$ or PM_{10}, particularly in urban areas. Fortunately, Aerosol Optical Depth (AOD) data from satellites offer opportunities to assess $PM_{10-2.5}$ more broadly. Our project leverages measurements from NASA's Terra satellite to estimate long-term $PM_{10-2.5}$ concentrations in six US urban areas (Los Angeles, CA; Chicago, IL; St. Paul, MN; Baltimore, MD; New York, NY; Winston-Salem, NC) for 2000–2012. We calibrated AOD (1 km^2 resolution) with EPA monitored PM_{10} and $PM_{2.5}$ levels daily using an area-specific mixed-modeling approach with land-use regression. We then used spatial smoothing in generalized additive mixed-models to predict daily PM_{10} and $PM_{2.5}$ when AOD was missing. $PM_{10-2.5}$ was estimated after taking the difference of spatially matched PM_{10} and $PM_{2.5}$ daily predictions. Model performance for our long-term average predictions was evaluated using leave-one-station-out cross-validation and compared to alternative, nearest-monitor and inverse distance weighting (IDW) approaches. Final long-term $PM_{10-2.5}$ predictions were well correlated with measured levels estimated from collocated $PM_{2.5}$ and PM_{10} sites in five of the six areas, with spatial CV R^2 ranging from 0.50 to 0.97. Only in Winston-Salem did the model have very little predictive ability (R^2: 0.34). All spatial predictions performed better than the nearest-monitor and IDW alternatives. In contrast, our final $PM_{10-2.5}$ predictions had poor temporal performance, with mean monitor-level CV R^2 ranging from 0.15 to 0.42. Given the superior performance of our spatial predictions compared to nearest-monitor and IDW alternatives and the high costs of field sampling, our results show the potential for combining AOD data with land-use regression to estimate long-term $PM_{10-2.5}$ concentrations in localized areas.

1. Introduction

Airborne particulate matter (PM) is physically diverse and is comprised of particles over a wide range of sizes (US EPA, 2009). In the epidemiology literature, the most common sizes studied are $PM_{2.5}$ (aerodynamic diameter $\leq$2.5 μm) and PM_{10} (aerodynamic diameter $\leq$10 μm). Relatively little

* Corresponding author. University of Michigan School of Public Health, 1415 Washington Heights, Ann Arbor, 48109-2029, MI, USA.
E-mail address: mpedde@umich.edu (M. Pedde).

https://doi.org/10.1016/j.atmosenv.2022.118945
Received 9 October 2021; Received in revised form 17 December 2021; Accepted 5 January 2022
Available online 13 January 2022

research has focused on $PM_{10-2.5}$ (aerodynamic diameter $\leq$10 μm and >2.5 μm), known as coarse particulate matter. A major challenge to epidemiologists in assessing the health risks of $PM_{10-2.5}$ has been a lack of monitors from which exposures can be estimated. Historically, only 1% of counties in the United States (US) have collocated PM_{10} and $PM_{2.5}$ monitors with which to estimate $PM_{10-2.5}$ (US EPA, 2009). This is especially problematic for studying the long-term health effects of $PM_{10-2.5}$ since $PM_{10-2.5}$ is more spatially variable than $PM_{2.5}$ or PM_{10} due to higher gravitational settling of larger particles (US EPA, 2009; US EPA, 2019; Wilson and Suh, 1997). Therefore, there is concern that the use of only a few central monitors for $PM_{10-2.5}$ will be insufficient to accurately reflect the exposures of individuals across a whole region, especially in urban areas, which often have considerable spatial variability in $PM_{10-2.5}$ concentrations (Lagudu et al., 2011; Pakbin et al., 2010; Sawvel et al., 2015; Thornburg et al., 2009; US EPA, 2019). As a result, only a handful of investigations have examined the health implications of long-term exposures to $PM_{10-2.5}$ in the US and many have suffered from statistical power issues, likely due to biases towards the null caused by measurement error (Adar et al., 2014).

Fortunately, data from National Aeronautics and Space Administration (NASA) satellites have created opportunities to assess PM concentrations at all locations across space. Aerosol optical depth (AOD) is a measure of light extinction by aerosol scattering and absorption in the atmospheric column, which is sampled continuously from space at a 1 km^2 resolution (Kloog et al., 2011; Nordio et al., 2013; Sorek-Hamer et al., 2016). The availability of these daily measurements, along with advancements in spatiotemporal prediction modeling, allows for the estimation of air pollution levels at fine-scale spatial and temporal resolution even where no monitoring stations exist (Kloog et al., 2011).

Previous research has shown good predictive ability using satellite data-based prediction models for $PM_{2.5}$ (cross-validation (CV) R^2: 0.7 to 0.9) in the US, Italy, Israel, and Switzerland (Kloog et al., 2011, 2012a, 2012b, 2015; Hu, 2009; Hu et al., 2014; Lee et al., 2016; Madrigano et al., 2013; McGuinn et al., 2016; de Hoogh et al., 2018). The same methods were used to predict PM_{10} with similar performance in Italy (CV R^2: 0.65 to 0.79; Nordio et al., 2013; Stafoggia et al., 2017; Stafoggia et al., 2019) and Israel (CV R^2: 0.79 to 0.92; Kloog et al., 2015; Shtein et al., 2018). Recently, one study used the abundant number of PM_{10} monitoring stations in Italy to predict both $PM_{2.5}$ and $PM_{10-2.5}$ concentrations using AOD and land-use data and found CV R^2 for annual averages ranging from 0.43 to 0.59 (Stafoggia et al., 2019). To date, however, no model for $PM_{10-2.5}$ has been developed in the US using satellite information and thus this modern source of data has not yet been used in epidemiology studies. Therefore, in this study, we use AOD measured on the NASA Terra satellite to calculate daily 1 km^2 resolution $PM_{10-2.5}$ predictions in six US urban areas.

2. Material and methods

2.1. Study domain

Our study domain included the six regions of the Multi-Ethnic Study of Atherosclerosis (MESA) (Bild et al., 2002), which represent diversity in terms of climate, geographical features, proximity to large water bodies, and urbanicity. To capture sufficient monitoring stations in these regions, we focused our models on the areas within 60 km of the centroids of Chicago, Illinois; New York, New York; and St. Paul, Minnesota; and within 80 km of the centroid of Baltimore, Maryland. For Los Angeles, California our study domain was based on the irregular recruitment area of study participants and the unique topology of the region. Our area extended from just west of Santa Monica to the San Jacinto mountain range on the east, and from San Fernando on the north to Irvine on the south, excluding the Santa Ana Mountains. The Winston-Salem, North Carolina study domain was roughly the area within 60 km of the city's centroid, although we extended the domain south to include additional monitoring sites in Charlotte and east to Raleigh (Fig. 1).

2.2. PM monitoring data

As our primary source of data to build and validate our models, we obtained daily (i.e., 24-h average) Federal Reference Method (FRM) monitoring data for $PM_{2.5}$ and PM_{10} mass for the years 2000 through 2012 from the US Environmental Protection Agency's (EPA) Air Quality System (AQS). We restricted our datasets to stations with at least 30 observations throughout the study period. In cases where multiple monitors for the same particle size were sited at the same location, we used data only from the primary monitor. Since PM_{10} measurements are reported to EPA at standard conditions[1] whereas $PM_{2.5}$ is reported at local conditions, we used temperature and pressure data (see 2.4.5) to convert reported PM_{10} to local conditions so that PM_{10} and $PM_{2.5}$ were on the same scale prior to calculating $PM_{10-2.5}$ concentrations (US EPA, 2009).

2.3. AOD satellite data

AOD data is sampled continuously from space at a 1 km^2 resolution using Moderate Resolution Imaging Spectroradiometer (MODIS) technology on the polar orbiting and sun-synchronous NASA Terra satellite (Levy et al., 2007; Remer et al., 2005). The AOD data are retrieved by NASA using the Multi Angle Implementation of Atmospheric Correction (MAIAC) algorithm, which begins by gridding MODIS measurements of L1B data to a fixed 1 × 1 km grid so that the same gridcell is observed over time. The MAIAC algorithm then uses time series analysis and a combination of pixel and image-based processing to improve accuracy of cloud detection, aerosol retrievals, and atmospheric correction (Lyapustin et al., 2011a, 2011b, 2012). Although newer satellites are now available, we used 2000–2012 AOD data collected on the Terra satellite because it was the only satellite in operation at the beginning of our study period.

2.4. Spatial and temporal predictors of $PM_{2.5}$ and PM_{10}

In addition to the satellite AOD observations, we also included many spatial and temporal predictors in our linear mixed effects hybrid prediction model. We used R statistical software version 3.6.1 (R, 2019) to generate all spatial and temporal predictors for each 1 × 1 km gridcell as detailed below.

2.4.1. Elevation

We estimated average gridcell elevation values using data from the USGS 3D Elevation Program (3DEP), which produces a satellite-based, seamless digital elevation model covering the conterminous US and Hawaii at a spatial resolution of 1/3 arc sec (approximately 10 m) (USGS, 2017).

2.4.2. Land use

We calculated the percentage of 15 different land use classes for each gridcell using raster data from the USGS National Land Cover Databases (NLCD) for years 2001, 2006, and 2011 (USGS, 2001; USGS, 2006; USGS, 2011). These data are measured at a 30-m resolution. The 2001 NLCD measures were assigned to gridcells for days in 2000 through mid-2003; 2006 NLCD measures were assigned to gridcells for days in mid-2003 through mid-2008, and; 2011 NLCD measures were assigned to gridcells for days in mid-2008 through 2012.

2.4.3. Normalized Difference Vegetation Index

We spatially and temporally matched monthly, 1 km^2 resolved vegetation data from the NASA Terra Moderate Resolution Imaging Spectroradiometer MOD13A3 version 6 Normalized Difference Vegetation Index (NDVI) (Didan, 2015) to study gridcells.

[1] EPA-defined standard conditions of temperature and pressure are 25 °C and 760 mm Hg, respectively.

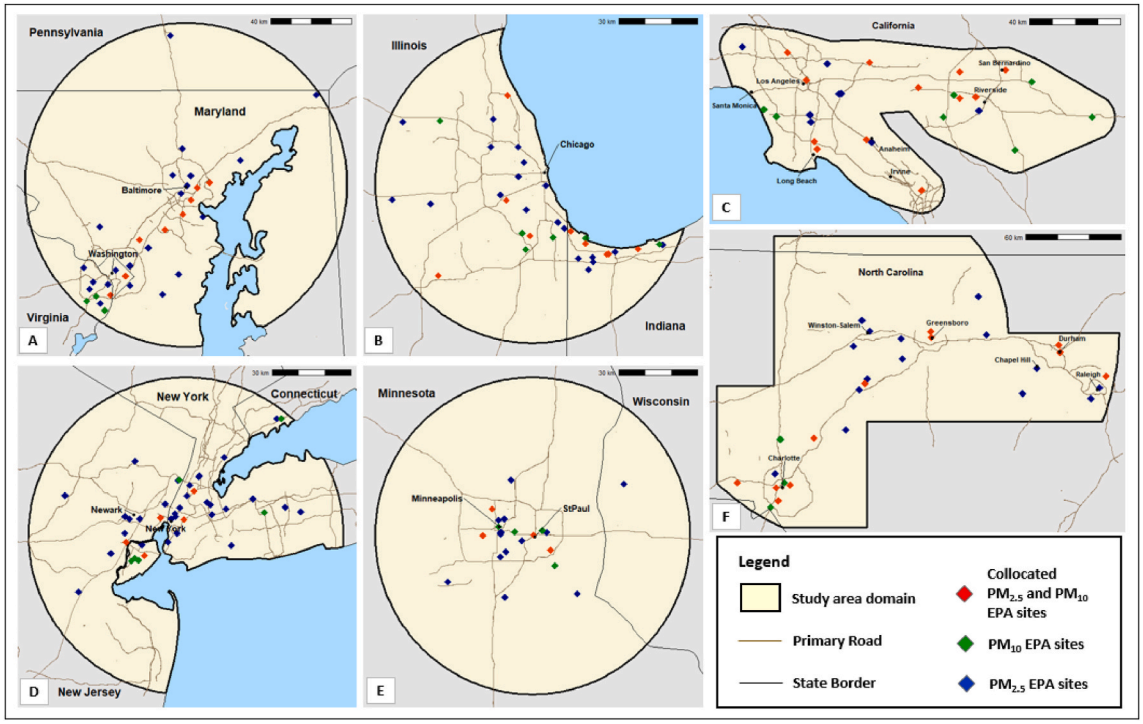

Fig. 1. Study areas and EPA monitor station locations for A) Baltimore, Maryland; B) Chicago, Illinois; C) Los Angeles, California; D) New York, New York; E) St. Paul, Minnesota; and F) Winston-Salem, North Carolina.

2.4.4. Planetary boundary layer

Using data from the European Centre for Medium-Range Weather Forecasts (ECMWF) ERA Interim Daily global atmospheric reanalysis model at a spatial resolution of 0.125° (~14 km) and 3-h temporal resolution (Dee et al., 2011), we estimated daily average planetary boundary layer (PBL) height by spatially and temporally matching daily averaged PBL to study gridcell centroids.

2.4.5. Meteorology

Meteorological data for air pressure, air temperature, evaporation, precipitable water, specific humidity, u-wind, v-wind, and visibility came from the National Oceanic and Atmospheric Administration's National Centers for Environmental Prediction North American Regional Reanalysis (NARR) dataset (Mesinger et al., 2006). This modeled data has a spatial resolution of approximately 0.3° (~32 km) and 3-h temporal resolution, which we averaged to the day and spatially and temporally matched to study gridcell centroids.

2.4.6. Population

We obtained US Census block-group total population counts and block-group shapefiles for the 2000 and 2010 Decennial censuses from the IPUMS National Historical Geographic Information System (NHGIS) (Manson et al., 2018). We then calculated two block-group spatially--weighted population measures: the first applied the 2000 Census-based population count to all days in years 2000–2004 and the 2010 Census-based population count to all days in 2005–2012 while the second linearly interpolated gridcell population for each year between the 2000 and 2010 Census values.

2.4.7. Roads and railways

We used primary and secondary road and railway feature data from the US Census TIGER/Line Shapefile online download system (US Census Bureau, 2012) to calculate the density of all primary and secondary roads (combined) in each gridcell. Additionally, we calculated the distance from each gridcell centroid to the nearest primary road, secondary road, and rail track.

2.4.8. Water bodies

Water feature data came from the USGS National Hydrography Dataset (USGS, 2019) (for both waterbody and water area categories). We calculated the distance from each gridcell centroid to the nearest water feature of any size and large water body (where we defined each city's large water body as follows: Chesapeake Bay for Baltimore; Lake Michigan for Chicago; Pacific Ocean for Los Angeles; Atlantic Ocean and Long Island Sound for New York; Lake Superior for St. Paul; and Atlantic Ocean for Winston-Salem).

2.5. Statistical methods

To estimate $PM_{10\text{-}2.5}$ concentrations, we used a previously developed spatiotemporal mixed effects modeling approach (Kloog et al., 2012a, 2014, 2015). This technique leveraged satellite AOD data to predict daily $PM_{2.5}$ and, separately, PM_{10}, at a 1 km^2 spatial resolution that we then used to calculate spatially resolved daily and long-term $PM_{10\text{-}2.5}$ concentrations via subtraction. Predicting $PM_{2.5}$ and PM_{10} separately, as opposed to predicting $PM_{10\text{-}2.5}$ directly, increased the amount of information used in the models since our study areas had many ground-level EPA monitoring sites that were not collocated. This choice also allowed for a more geographically diverse set of monitoring stations to inform our predictions, which will then better represent the areas where participants in future health analyses reside. All statistical modeling was done using R software version 3.5.0 (R, 2018) and all maps were created using R software 3.6.1 (R, 2019).

2.5.1. PM predictions

In the first stage of our analysis, we fit a calibration model (1), which predicts measured PM as a function of AOD for all ground-level measurements of PM with an available AOD value within 1.1 km. We constructed individual models for each city and particle size ($PM_{2.5}$ and PM_{10}):

$$PM_{ij} = (\alpha + \mu_j) + (\beta_1 + \nu_j)AOD_{ij} + \sum_{m=1}^{10} \gamma_{1_m} X_{1_{m_{ij}}} + \sum_{m=1}^{24} \gamma_{2_m} X_{2_{m_i}} + \varepsilon_{ij} \quad (1)$$

Where: PM_{ij} is the measured $PM_{2.5}$ or PM_{10} concentration in a city at site i on day j; α is the fixed intercept and μ_j is the day-specific random intercept; β_1 is the fixed slope for AOD while ν_j is the day-specific random slope for AOD. AOD_{ij} is the AOD value for the gridcell corresponding to site i on day j; $X_{1_{m_{ij}}}$ is the mth spatiotemporal predictor in the gridcell corresponding to site i on day j (i.e., vegetation, eight meteorology predictors, and PBL height) and γ_{1_m} is the slope of the mth spatiotemporal predictor; $X_{2_{m_i}}$ is the mth spatial predictor in the gridcell corresponding to site i (i.e., elevation, two population measures, fifteen land use categories, road density, and proximity to: primary road, secondary road, railroad, any water body, and large water body) and γ_{2_m} is the slope of the mth spatial predictor.

Since AOD data can become unreliable with cloud contamination, snow-cover, high surface brightness, and other factors, we excluded observations with an AOD uncertainty value ≤ 0 or ≥ 0.04, per MAIAC guidelines. Observations where the gridcell included $\geq 5\%$ open water (based on the land use data) were also excluded since AOD data can be similarly unreliable near water surfaces. We additionally excluded observations where the AOD and/or the PM value was at or below the city-specific 1st percentile or at or above the city-specific 99th percentile to reduce the potential influence of outlier values on these first stage calibration models.[2] Finally, since many of the land use categories had little variation within the modeling domains, we excluded predictors where the value of the 25th percentile was equal to the 75th percentile.[3]

Within this cleaned dataset, AOD can be missing not-at-random due to factors such as levels of cloud and snow coverage even when they are valid based on the AOD uncertainty value described above. These factors can also be correlated with PM levels since, for example, cloud coverage can change deposition rates, vertical distributions, chemical composition, and rates of secondary aerosol formation (Belle et al., 2017; Christiansen et al., 2020; Christopher and Gupta, 2010). This could impact the calibration stage regression coefficients in equation (1) and therefore the calibration model-based predictions. To address this potential bias, we created inverse probability weights (IPW) to up-weight observed gridcell-days that share characteristics with days that have more missing AOD data. The weights were calculated by fitting the following logistic regression model (2) separately for each year and each city for the probability, p, of having a non-missing AOD value for gridcell i on day j:

$$\ln\left(\frac{p}{1-p}\right) = \beta_0 + \beta_1 Elevation_i + \beta_2 PBL_{ij} + \beta_3 Temperature_{ij} + \sum_{k=4}^{14} \beta_k I(Month)_j \quad (2)$$

Using weights of $\frac{1}{p}$ derived from (2), we then used backward selection with the Akaike Information Criterion (AIC) to select the fixed effects used in each calibration model (1). This generated city- and particle size fraction-specific calibration models which we used to predict PM for gridcell-days with available AOD data (including the IPW weighting).

As mentioned earlier, AOD data are often missing. Across the six study areas and throughout our study period of interest, AOD missingness ranged from 54% in Los Angeles to 75% in St. Paul, consistent with previous work (Just et al., 2015; Stafoggia et al., 2019). Therefore, to predict PM in gridcell-days without available AOD data, we fit the following generalized additive mixed model, which uses average regional measured PM and a smooth function of the gridcell centroid coordinates, to predict the AOD-based PM estimates that were calculated with the model (1) fit:

$$PredPM_{ij} = (\alpha + \mu_i) + (\beta_1 + \nu_i) MPM_{ij} + s(lat_i, lon_i)_{k(j)} + \varepsilon_{ij} \quad (3)$$

$PredPM_{ij}$ is the predicted PM calculated with calibration model (1) for gridcell-days with available AOD data; α is the fixed intercept and μ_i is the gridcell-specific random intercept; MPM_{ij} is the mean PM from all EPA sites within 60 km of the centroid of gridcell i on day j; β_1 is the fixed slope on MPM while ν_i is the gridcell-specific random slope for MPM; $s(lat_i, lon_i)_{k(j)}$ is a thin plate spline of the latitude and longitude of the centroid of gridcell i for the season, k(j), in which day j falls (i.e., we fit a separate thin plate spline smoothing function for each season in the study period).

Our final $PM_{2.5}$ and PM_{10} predictions were created by selecting – by day and gridcell – the 'best' available PM measure. We prioritized EPA measured PM values first. If unavailable, we selected calibration-based model predictions followed finally by the smoothing model PM predictions. This approach results in a full-coverage prediction dataset for each city for each PM size fraction for days with and without AOD measurements. We then estimated $PM_{10\text{-}2.5}$ concentrations as the difference between PM_{10} and $PM_{2.5}$ concentrations.

2.5.2. Model evaluation

We performed 'leave-one-station-out' (LOSO) cross-validation (CV) to assess the performance of our models. Specifically, to generate the calibration model CV predictions, we repeatedly left out one of the N total PM monitors in each city and re-fit the AIC-chosen calibration model on only data from the N-1 remaining PM stations. We then used the model fit from the N-1 sites to predict PM at the held-out site. Conceptually, this approach assesses the performance of the calibration models vs. observed values at an unobserved location. The smoothing model CV predictions were generated by recursively fitting the smoothing model on the predicted values from the calibration model fit from the N-1 sites.

We separately evaluated the calibration CV predictions and our final CV predictions, where the latter were selected from the 'best' of either the calibration model CV or smoothing model CV predictions. Both were evaluated for all three size fractions and against all available EPA PM monitoring data throughout the study period (i.e., for PM with and without paired available AOD data, as appropriate). Since the EPA does not provide publicly available $PM_{10\text{-}2.5}$ data, we created a validation dataset of daily and long-term average $PM_{10\text{-}2.5}$ concentrations by subtracting $PM_{2.5}$ from PM_{10} measured at EPA FRM monitoring stations with collocated monitors.

To evaluate our CV predictions, we regressed the spatially and temporally paired daily observed concentrations on the daily CV predicted concentrations and summarized the R^2, intercept, and slope; we also calculated the root mean square error (RMSE) of the predictions. To examine the ability of our models to estimate the spatial variation in PM concentrations, we regressed our CV predictions against observed concentrations averaged over the full study-period and again summarized the R^2, intercept, and slope, and again calculated the RMSE. To isolate and assess the temporal performance of the models, we calculated the overall R^2 for our CV predictions separately for each EPA monitoring site. We then generated summary statistics (i.e., mean and standard deviation) of monitor-specific R^2, intercept, slope, and RMSE values, separately for each city and particle size.

In three of our six study areas we additionally compared our final AOD-based $PM_{10\text{-}2.5}$ predictions to 2-week $PM_{10\text{-}2.5}$ samples taken during both the summer and winter seasons for the MESA Coarse study (Zhang et al., 2014). Daily AOD-based predictions were spatially and temporally linked to the external measurements and averaged over the corresponding 2-week sampling periods. We used the correlation between our predictions and the measurements, separately for each city, to assess the performance of our predictions relative to the out-of-sample measurements.

[2] The St. Paul PM_{10} analysis used thresholds of 2.5th and 97.5th percentiles to improve the model fit.

[3] The calibration model for Chicago $PM_{2.5}$ excluded predictors where the value of the 1st percentile was equal to the 99th percentile to improve model fit.

2.5.3. Alternative modeling approaches

In secondary analyses, we evaluated three alternate approaches for estimation of $PM_{10-2.5}$: two to compare to our model's spatial performance and one to compare to our model's temporal performance. The first alternative spatial approach was a nearest monitor analysis, which is used in some of the $PM_{10-2.5}$ long-term health effects literature (Lipsett et al., 2006; Miller et al., 2007; Chen et al., 2015). The second alternative spatial approach was inverse distance weighting (IDW) using weights of squared inverse distance. For both alternative approaches we repeatedly left out one collocated $PM_{2.5}$ and PM_{10} site at a time and assigned it – by day – the $PM_{10-2.5}$ concentration from the collocated $PM_{2.5}$ and PM_{10} EPA site that was geographically closest to the held-out site (for the nearest monitor approach) or the $PM_{10-2.5}$ prediction from the IDW interpolation of all other collocated $PM_{2.5}$ and PM_{10} EPA sites in the study area (for the IDW approach). We then compared the study-period average $PM_{10-2.5}$ concentrations at the held-out sites, separately, to the $PM_{10-2.5}$ estimates from each of the two alternative spatial approaches and reported spatial R^2 values, intercepts, slopes, and RMSE values, separately for each city.

We similarly determined whether our $PM_{10-2.5}$ prediction approach performed better temporally than a regional average $PM_{10-2.5}$ measurement, which is an alternative method commonly used in the $PM_{10-2.5}$ health effects time series literature (Chen et al., 2004; Lin et al., 2005; Malig et al., 2013; Peng et al., 2008; Rodopoulou et al., 2014; Stafoggia et al., 2013; US EPA, 2019; Zhao et al., 2017). Specifically, for each daily measured $PM_{10-2.5}$ concentration at a given collocated $PM_{2.5}$ and PM_{10} site, we calculated the daily average $PM_{10-2.5}$ value from all other collocated $PM_{2.5}$ and PM_{10} sites in the study area except itself for that day. We then compared the daily $PM_{10-2.5}$ concentrations at the held-out site to the daily region-average $PM_{10-2.5}$ concentrations, separately for each held-out monitoring site, and reported the mean and standard deviation of monitor-specific reported R^2 values, intercepts, slopes, and RMSE values, separately for each city.

3. Results

Fig. 1 shows the study area for each of the six study regions, including the locations of the $PM_{2.5}$, PM_{10}, and collocated $PM_{2.5}$ and PM_{10} EPA monitoring stations used in the analysis. Notably, each city had a higher frequency of $PM_{2.5}$ sampling compared with PM_{10} (roughly one out of three days for $PM_{2.5}$ and one out of six days for PM_{10}) and a larger number of $PM_{2.5}$ samplers (Table 1). The number of PM sites used in this analysis differed by city, with New York having the most $PM_{2.5}$ samplers (N = 37) and Los Angeles having the most PM_{10} samplers (N = 19). St. Paul had the fewest $PM_{2.5}$ (N = 17) and PM_{10} (N = 8) samplers. The number of unique collocated $PM_{10-2.5}$ sites in each city throughout the study period ranged from 4 in St. Paul to 12 in Los Angeles (Table 1). Based on monitoring data, we observed that the Los Angeles study region had the highest mean concentrations for both $PM_{2.5}$ (16.7 $\mu g/m^3$) and PM_{10} (35.6 $\mu g/m^3$) of all six areas. In contrast, St. Paul had the lowest mean $PM_{2.5}$ concentration (8.6 $\mu g/m^3$) and Baltimore had the lowest mean PM_{10} concentration (20.4 $\mu g/m^3$). Mean $PM_{10-2.5}$ concentrations at collocated sites throughout the study period ranged from 6.3 $\mu g/m^3$ in Winston-Salem to 20.7 $\mu g/m^3$ in Los Angeles.

In our calibration models that predicted PM based on AOD measurements, we found that AOD was consistently and strongly positively associated with $PM_{2.5}$ in all six areas and with PM_{10} in three of the cities but not in the more northern cities of Chicago, St. Paul, and New York (Table A.2). Meteorological factors, elevation, land use development level, and daily average PBL were the factors most commonly predictive of $PM_{2.5}$, while the vertical wind component, population, and humidity were most commonly predictive of PM_{10} (Table A.2).[4] As shown in Table 2, we had strong performance for predicting long-term average $PM_{10-2.5}$ – our particle size of primary interest – based on measured AOD. Our spatial CV R^2 was greater than 0.6 in four of our six cities (i.e., Baltimore, Los Angeles, New York, and St. Paul). The spatial CV R^2 was also good in Chicago at 0.57 but poor for Winston-Salem at 0.25. In all sites except Winston-Salem these $PM_{10-2.5}$ spatial R^2 were consistent with, if not better than, $PM_{2.5}$ or PM_{10} alone, which ranged from 0.46 in Chicago to 0.81 in New York for $PM_{2.5}$ and from 0.52 in Chicago to 0.95 in New York for PM_{10}. In contrast, we had poor predictive performance overall due to poor predictive power of $PM_{10-2.5}$ temporal variation. In fact, the model performance was much worse temporally for $PM_{10-2.5}$ (average temporal CV R^2s from 0.10 to 0.43) than for either $PM_{2.5}$ (average temporal CV R^2s from 0.69 to 0.83) or PM_{10} (average temporal CV R^2s from 0.52 to 0.69) in all six cities.

Validation results of our final predictions for all three size fractions are shown in Table 3. As with our calibration models, our final $PM_{10-2.5}$ models had excellent spatial performance in Baltimore, Los Angeles, New York, and St. Paul, with CV R^2s ranging from 0.70 to 0.97. Chicago again had moderate $PM_{10-2.5}$ spatial performance (CV R^2: 0.50) and Winston-Salem had a low spatial CV R^2 of 0.34. Temporal performance remained low for our final $PM_{10-2.5}$ predictions, with mean CV R^2 ranging from 0.15 to 0.42.

The spatial performance of our AOD-based models was substantially better than both alternate spatial approaches, both of which performed poorly in all six cites (Table 4). In contrast, the alternate temporal approach of a city mean performed slightly better than the temporal component of our AOD based predictions across the study areas (based on mean CV R^2) although in general, the results were still poor. When compared to two-week samples collected from residential areas in the MESA Coarse project, our satellite-based predictions showed good correlations with measurements in St. Paul (ρ: 0.43) and Chicago (ρ: 0.63), but poor correlations in Winston-Salem (ρ: −0.11).

Maps of our final $PM_{2.5}$, PM_{10}, and $PM_{10-2.5}$ predictions averaged over the study period are shown in Fig. 2 for each area. In general, $PM_{2.5}$ predicted concentrations were highest along major roadways and in the downtown areas of all six cities, while PM_{10} and $PM_{10-2.5}$ predictions exhibited similar but weaker roadway and downtown spatial patterns.

Summary statistics for the final long-term average predictions, by city and particle size, are shown in Table 5. Mean study area long-term average $PM_{2.5}$ ranged from 7.9 $\mu g/m^3$ in Chicago to 12.0 $\mu g/m^3$ in Winston-Salem while PM_{10} ranged from 11.5 $\mu g/m^3$ in Baltimore to 37.7 $\mu g/m^3$ in New York; Baltimore had the lowest mean long-term average $PM_{10-2.5}$ predictions (2.1 $\mu g/m^3$) while New York had the highest (28.4 $\mu g/m^3$).

4. Discussion

We used spatiotemporal mixed effects models with satellite AOD data to predict $PM_{10-2.5}$ at a 1 km^2 resolution in six metropolitan areas across the US. This extends earlier work which successfully developed and applied this approach throughout the eastern US, Italy, and Israel for $PM_{2.5}$ (Kloog et al., 2011, 2012a, 2012b, 2015; Hu, 2009; Madrigano et al., 2013; McGuinn et al., 2016) and in Italy and Israel for PM_{10} (Nordio et al., 2013; Stafoggia et al., 2017, 2019; Kloog et al., 2015; Shtein et al.,

[4] Although elevation was a selected fixed effect in the Baltimore PM_{10} calibration model, given the topological characteristics of that region compared to the locations of PM_{10} monitors, using elevation in the AOD-based predictions resulted in a large fraction of negative PM_{10} predictions. We therefore re-performed AIC backward selection after excluding elevation as a predictor for consideration.

Table 1
Summary statistics of daily $PM_{2.5}$, PM_{10}, and $PM_{10-2.5}$ concentrations (μg/m^3) used in calibration models, measured at EPA air quality monitoring stations in six US metropolitan areas for the period 2000–2012.

City	Particle Size	Number of Sites	Number of Observations	Mean	Median	Min	Max	IQR
Baltimore	$PM_{2.5}$	30	11,587	12.2	10.6	3.2	38.2	8.2
	PM_{10}	13	1382	20.4	18	4	60	13
	$PM_{10-2.5}$	8	816	9.2	6.4	−20.5	73.4	8.4
Chicago	$PM_{2.5}$	28	8309	12.9	11.5	3.2	37.1	8.7
	PM_{10}	15	1934	23.5	22	6	61	15
	$PM_{10-2.5}$	9	1035	10.5	8.5	−13.6	94.0	9.1
Los Angeles	$PM_{2.5}$	22	13,491	16.7	14	2.8	59.3	11
	PM_{10}	19	4513	35.6	33	7	95	22
	$PM_{10-2.5}$	12	2950	20.7	18.0	−19.7	123.2	14.7
New York	$PM_{2.5}$	37	11,340	11.1	9.1	2.7	38.5	8.3
	PM_{10}	11	787	24.8	21	7	78	18
	$PM_{10-2.5}$	5	369	12.4	9.5	−10.4	70.8	10.0
St. Paul	$PM_{2.5}$	17	3898	8.6	7.6	2.2	26.9	5.3
	PM_{10}	8	960	25.6	24	9	57	15
	$PM_{10-2.5}$	4	394	17.1	15.2	1.4	47.9	11.5
Winston-Salem	$PM_{2.5}$	27	15,110	12.7	11.5	0	84.5	8.2
	PM_{10}	15	2361	20.8	19	1	99	12
	$PM_{10-2.5}$	11	1491	6.3	5.8	−10.9	49.4	4.5

Table 2
Cross-validated performance of calibration models for $PM_{2.5}$, PM_{10}, and $PM_{10-2.5}$ predictions by study area and particle size.

City	Particle Size	Overall				Spatial				Temporal[c]			
		R^2	RMSE[b]	Intercept[a]	Slope[a]	R^2	RMSE[b]	Intercept[a]	Slope[a]	R^2	RMSE	Intercept	Slope
Baltimore	$PM_{2.5}$	0.79	3.45	−0.23 (0.07)	1.03 (0.005)	0.65	0.70	2.73 (1.38)	0.79 (0.11)	0.83 (0.07)	3.21 (0.9)	−0.43 (1.13)	1.05 (0.07)
	PM_{10}	0.54	8.23	−1.21 (0.58)	1.08 (0.03)	0.69	3.17	−3.56 (5.02)	1.19 (0.24)	0.62 (0.14)	7.22 (3.35)	−1.71 (4.92)	1.07 (0.19)
	$PM_{10-2.5}$	0.16	9.01	2.86 (0.6)	0.73 (0.06)	0.65	3.18	−1.59 (3.21)	1.25 (0.37)	0.1 (0.07)	7.8 (3.83)	4.41 (4.2)	0.42 (0.27)
Chicago	$PM_{2.5}$	0.75	3.59	−0.11 (0.09)	1.02 (0.01)	0.46	0.95	3.93 (1.91)	0.7 (0.15)	0.8 (0.11)	3.23 (0.97)	−0.29 (1.13)	1.03 (0.07)
	PM_{10}	0.48	8.56	1.54 (0.55)	0.94 (0.02)	0.52	3.40	8.06 (4.4)	0.68 (0.18)	0.53 (0.15)	8.7 (2.01)	−3.45 (12.09)	1.13 (0.39)
	$PM_{10-2.5}$	0.23	7.87	4.36 (0.42)	0.68 (0.04)	0.57	3.03	4.12 (2.63)	0.71 (0.23)	0.28 (0.17)	8.14 (2.63)	0.56 (8.82)	0.94 (0.47)
Los Angeles	$PM_{2.5}$	0.66	6.86	−0.26 (0.12)	1.03 (0.01)	0.56	2.21	2.13 (3.07)	0.92 (0.18)	0.69 (0.09)	6.93 (2.5)	−0.27 (2.83)	1.05 (0.17)
	PM_{10}	0.56	12.18	−0.64 (0.5)	1.02 (0.01)	0.62	4.43	2.71 (6.44)	0.94 (0.18)	0.56 (0.12)	12.12 (4.05)	−2.34 (10.2)	1.05 (0.3)
	$PM_{10-2.5}$	0.43	9.70	2.99 (0.42)	0.83 (0.02)	0.74	2.70	3.23 (3.33)	0.82 (0.15)	0.43 (0.15)	9.16 (1.97)	0.85 (9.13)	0.88 (0.38)
New York	$PM_{2.5}$	0.76	3.96	−0.31 (0.07)	1.04 (0.01)	0.81	0.77	−0.28 (1.01)	1.05 (0.09)	0.78 (0.12)	3.97 (1.6)	−0.4 (0.85)	1.05 (0.07)
	PM_{10}	0.62	9.61	−1.07 (0.79)	1.06 (0.03)	0.95	1.48	−3.28 (2.11)	1.14 (0.09)	0.63 (0.17)	8.45 (2.73)	−1.03 (6.22)	1.01 (0.23)
	$PM_{10-2.5}$	0.35	8.71	1.22 (0.92)	0.86 (0.06)	0.96	1.70	−2.42 (1.75)	1.1 (0.13)	0.35 (0.19)	7.23 (2.74)	−3.68 (16.3)	0.91 (0.97)
St. Paul	$PM_{2.5}$	0.73	2.71	−0.23 (0.1)	1.05 (0.01)	0.49	0.82	0.06 (2.34)	1.03 (0.27)	0.76 (0.15)	2.84 (1.86)	−0.41 (0.58)	1.08 (0.08)
	PM_{10}	0.50	9.04	−1.53 (0.91)	1.08 (0.03)	0.88	1.55	−2.54 (4.4)	1.11 (0.17)	0.52 (0.16)	8.17 (2.78)	−1.74 (1.54)	1.07 (0.08)
	$PM_{10-2.5}$	0.40	8.34	1.52 (1.04)	0.89 (0.05)	0.82	2.03	1.88 (5.4)	0.85 (0.28)	0.35 (0.15)	8.27 (2.22)	0.82 (2.69)	0.91 (0.17)
Winston-Salem	$PM_{2.5}$	0.80	2.94	−0.26 (0.06)	1.02 (0.004)	0.93	0.65	−1.04 (0.81)	1.08 (0.06)	0.81 (0.07)	2.86 (0.68)	−0.3 (0.73)	1.02 (0.05)
	PM_{10}	0.67	5.87	−0.32 (0.33)	1.04 (0.02)	0.72	2.02	0.54 (3.53)	0.98 (0.17)	0.69 (0.09)	5.27 (1.45)	−0.4 (3.57)	1.01 (0.2)
	$PM_{10-2.5}$	0.19	4.68	3.38 (0.19)	0.46 (0.02)	0.25	1.88	4.04 (1.36)	0.34 (0.2)	0.22 (0.15)	4.46 (1.18)	2.43 (1.85)	0.55 (0.3)

[a] Shown as parameter estimate ± standard error from a linear regression of observations versus predictions.
[b] Root of the mean squared error.
[c] Shown as the mean (standard deviation) of the statistic, across all monitor-level results from linear regressions of observations versus predictions.

2018). Overall, our final predictions captured the long-term spatial patterns of $PM_{10-2.5}$ very well in four of our study areas (CV R^2 ranging from 0.70 in Los Angeles to 0.97 New York), well in one area (CV R^2 of 0.50 in Chicago), and modestly in one area (CV R^2 of 0.34 in Winston-Salem). In all six study areas, our predictions had substantially better spatial performance than both a simple nearest-monitor approach and an IDW approach. Given that urban areas often have considerable spatial variability in $PM_{10-2.5}$ concentrations (Lagudu et al., 2011; Pakbin et al., 2010; Sawvel et al., 2015; Thornburg et al., 2009; US EPA, 2019), our results show the benefits of using satellite-based AOD data for assessing long-term $PM_{10-2.5}$ concentrations for epidemiological health studies.

This research adds to the literature as one of only a handful of models to predict $PM_{10-2.5}$ concentrations for use in long-term air pollution epidemiological studies. This is particularly true for the US where – to

Table 3
Cross-validated performance of final 'best' models for $PM_{2.5}$, PM_{10}, and $PM_{10-2.5}$ predictions by study area and particle size.

City	Particle Size	Overall				Spatial				Temporal[c]			
		R^2	RMSE[b]	Intercept[a]	Slope[a]	R^2	RMSE[b]	Intercept[a]	Slope[a]	R^2	RMSE	Intercept	Slope
Baltimore	$PM_{2.5}$	0.87	3.11	−2.09 (0.03)	1.2 (0.002)	0.75	0.87	0.95 (1.34)	0.96 (0.11)	0.88 (0.04)	3.05 (0.67)	−1.95 (1.2)	1.19 (0.08)
	PM_{10}	0.59	7.53	−4.01 (0.32)	1.18 (0.01)	0.74	2.36	0.65 (3.58)	0.96 (0.17)	0.67 (0.1)	6.53 (2.54)	−6.21 (6.01)	1.26 (0.22)
	$PM_{10-2.5}$	0.23	7.73	0.7 (0.29)	0.8 (0.03)	0.74	2.14	−0.02 (1.82)	0.89 (0.21)	0.15 (0.08)	6.46 (2.77)	0.91 (2.02)	0.65 (0.4)
Chicago	$PM_{2.5}$	0.81	4.01	−3.83 (0.05)	1.34 (0.003)	0.40	1.16	6.32 (1.86)	0.58 (0.14)	0.85 (0.06)	3.76 (0.68)	−4.11 (1.54)	1.36 (0.1)
	PM_{10}	0.51	8.69	−1.2 (0.28)	1.03 (0.01)	0.50	3.72	10.16 (3.65)	0.56 (0.15)	0.57 (0.07)	8.58 (1.56)	−7.42 (8.06)	1.29 (0.2)
	$PM_{10-2.5}$	0.30	7.62	2.38 (0.18)	0.68 (0.02)	0.50	3.48	4.51 (1.84)	0.46 (0.17)	0.36 (0.11)	7.27 (1.49)	−0.75 (3.9)	0.99 (0.16)
Los Angeles	$PM_{2.5}$	0.71	6.12	−2.32 (0.07)	1.15 (0.004)	0.41	2.21	5.57 (3)	0.69 (0.18)	0.76 (0.08)	6.08 (1.31)	−2.87 (3.03)	1.21 (0.21)
	PM_{10}	0.50	15.94	−11.16 (0.42)	1.31 (0.01)	0.57	4.39	6.3 (6.06)	0.82 (0.17)	0.56 (0.13)	14.92 (7.94)	−16.52 (19.46)	1.44 (0.53)
	$PM_{10-2.5}$	0.41	11.45	−1.73 (0.3)	1 (0.01)	0.70	3.34	4.6 (3.04)	0.69 (0.14)	0.42 (0.16)	10.74 (2.92)	−4.55 (10.77)	1.08 (0.46)
New York	$PM_{2.5}$	0.85	3.40	−2.03 (0.03)	1.22 (0.002)	0.66	1.07	−1.39 (1.76)	1.16 (0.15)	0.86 (0.06)	3.38 (0.71)	−1.98 (0.71)	1.2 (0.08)
	PM_{10}	0.65	9.35	−6.47 (0.45)	1.28 (0.02)	0.92	2.16	−5.46 (2.86)	1.25 (0.12)	0.65 (0.1)	8.05 (3.13)	−5.64 (7.6)	1.21 (0.3)
	$PM_{10-2.5}$	0.38	8.46	−1.23 (0.46)	1.01 (0.03)	0.97	2.32	−5.14 (1.62)	1.32 (0.13)	0.22 (0.05)	7.78 (3.45)	−1 (5.46)	0.79 (0.51)
St. Paul	$PM_{2.5}$	0.83	3.28	−2.99 (0.05)	1.41 (0.01)	0.35	0.94	3.57 (2.26)	0.69 (0.24)	0.83 (0.08)	3.26 (0.83)	−3.13 (0.67)	1.41 (0.08)
	PM_{10}	0.49	9.42	−4.01 (0.46)	1.13 (0.02)	0.84	1.60	4.9 (3.68)	0.79 (0.14)	0.52 (0.08)	8.95 (1.86)	−6.43 (4.41)	1.21 (0.14)
	$PM_{10-2.5}$	0.35	9.82	−0.95 (0.59)	0.93 (0.03)	0.85	3.21	3.32 (3.67)	0.68 (0.2)	0.33 (0.06)	9.59 (1.99)	−4.72 (6.67)	1.07 (0.29)
Winston-Salem	$PM_{2.5}$	0.89	2.36	−1.8 (0.03)	1.14 (0.002)	0.93	0.58	−0.96 (0.8)	1.08 (0.06)	0.89 (0.03)	2.32 (0.41)	−1.78 (0.86)	1.14 (0.05)
	PM_{10}	0.75	4.84	−2.08 (0.18)	1.11 (0.01)	0.77	1.72	1.36 (2.85)	0.93 (0.14)	0.77 (0.06)	4.46 (1.1)	−2.8 (3.03)	1.13 (0.14)
	$PM_{10-2.5}$	0.35	3.82	2.18 (0.1)	0.63 (0.01)	0.34	1.79	3.89 (1.07)	0.34 (0.16)	0.4 (0.08)	3.78 (0.85)	0.87 (2.03)	0.79 (0.21)

[a] Shown as parameter estimate ± standard error from a linear regression of observations versus predictions.
[b] Root of the mean squared error.
[c] Shown as the mean (standard deviation) of the statistic, across all monitor-level results from linear regressions of observations versus predictions.

Table 4
$PM_{10-2.5}$ model evaluation by study area using A) our AOD-based approach (final model CV) vs. two alternative spatial approaches (nearest monitor and inverse distance weighting); B) our AOD-based approach (final model CV) vs. an alternative temporal approach (city-average).

A	AOD-Based Approach				Alternative Spatial Approach: Nearest Co-Located Site				Alternative Spatial Approach: Inverse Distance Weighting			
City	R^2	RMSE[b]	Intercept[a]	Slope[a]	R^2	RMSE[b]	Intercept[a]	Slope[a]	R^2	RMSE[b]	Intercept[a]	Slope[a]
Baltimore	0.74	2.14	−0.02 (1.82)	0.89 (0.21)	0.03	4.44	12.66 (14.38)	−0.67 (1.66)	0.27	4.78	21.18 (9.67)	−1.72 (1.15)
Chicago	0.50	3.48	4.51 (1.84)	0.46 (0.17)	0.02	4.02	7.44 (3.78)	0.15 (0.4)	0.04	3.31	5.75 (5.89)	0.35 (0.65)
Los Angeles	0.70	3.34	4.6 (3.04)	0.69 (0.14)	0.23	4.56	8.49 (6.25)	0.52 (0.3)	0.14	4.22	6.27 (9.91)	0.65 (0.51)
New York	0.97	2.32	−5.14 (1.62)	1.32 (0.13)	0.57	9.30	21.32 (6.11)	−1.13 (0.56)	0.67	7.81	31.63 (9.02)	−2.23 (0.9)
St. Paul	0.85	3.21	3.32 (3.67)	0.68 (0.2)	0.14	3.93	9.76 (10.35)	0.37 (0.64)	0.02	3.84	12.04 (17.15)	0.23 (1.08)
Winston-Salem	0.34	1.79	3.89 (1.07)	0.34 (0.16)	0.04	2.35	7.06 (1.78)	−0.15 (0.26)	0.03	1.93	7.37 (2.43)	−0.2 (0.37)

B	AOD-Based Approach[c]				Alternative Temporal Approach: Measured City Average			
City	R^2	RMSE	Intercept	Slope	R^2	RMSE	Intercept	Slope
Baltimore	0.15 (0.08)	6.46 (2.77)	0.91 (2.02)	0.65 (0.4)	0.26 (0.19)	7.79 (4.09)	3.48 (3.26)	0.43 (0.15)
Chicago	0.36 (0.11)	7.27 (1.49)	−0.75 (3.9)	0.99 (0.16)	0.38 (0.06)	7.22 (1.36)	1.73 (3.09)	0.81 (0.15)
Los Angeles	0.42 (0.16)	10.74 (2.92)	−4.55 (10.77)	1.08 (0.46)	0.59 (0.16)	10.41 (3.08)	1.39 (5.27)	0.95 (0.45)
New York	0.22 (0.05)	7.78 (3.45)	−1 (5.46)	0.79 (0.51)	0.2 (0.05)	10.35 (3.82)	4.64 (3.19)	0.61 (0.51)
St. Paul	0.33 (0.06)	9.59 (1.99)	−4.72 (6.67)	1.07 (0.29)	0.38 (0.14)	10.79 (1.53)	4.95 (2.6)	0.72 (0.2)
Winston-Salem	0.4 (0.08)	3.78 (0.85)	0.87 (2.03)	0.79 (0.21)	0.38 (0.14)	3.84 (1.09)	1.61 (1.47)	0.7 (0.22)

[a] Shown as parameter estimate ± standard error from a linear regression of observations versus predictions.
[b] Root of the mean squared error.
[c] Shown as the mean (standard deviation) of the statistic, across all monitor-level results from linear regressions of observations versus predictions.

our knowledge – only two groups have generated $PM_{10-2.5}$ exposure predictions that have been used in health studies (US EPA, 2019). Notably, neither has taken advantage of the additional information AOD provides when conducting $PM_{10-2.5}$ spatiotemporal pollution prediction modeling. Previously, our group used intensive $PM_{10-2.5}$ monitoring campaigns as part of the MESA Coarse study (Zhang et al., 2014) to predict spatial patterns of $PM_{10-2.5}$ using land use regression methods in three of the six cities studied here. While our model performance using

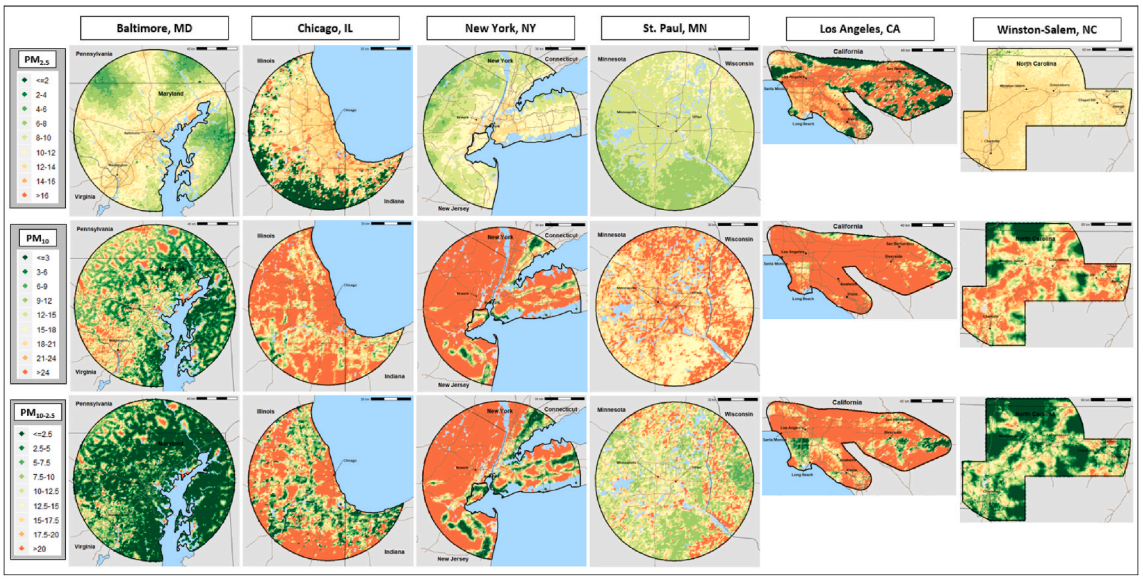

Fig. 2. Maps of long-term average PM predictions (2000–2012), by particle size and study area.

Table 5
Summary statistics of final long-term average (2000–2012) $PM_{2.5}$, PM_{10}, and $PM_{10\text{-}2.5}$ predictions (μg/m^3), by study area and particle size.

City	Particle Size	Mean (SD)	25th Percentile	75th Percentile
Baltimore	$PM_{2.5}$	9.6 (2.3)	8.0	11.4
	PM_{10}	11.5 (7.6)	5.6	16.7
	$PM_{10\text{-}2.5}$	2.1 (7.1)	−3.2	6.7
Chicago	$PM_{2.5}$	7.9 (10.3)	7.0	13.4
	PM_{10}	26.2 (9.5)	19.7	31.8
	$PM_{10\text{-}2.5}$	18.8 (14.0)	9.2	26.4
Los Angeles	$PM_{2.5}$	8.7 (16.2)	4.0	17.2
	PM_{10}	34.9 (11.6)	28.1	43.0
	$PM_{10\text{-}2.5}$	26.0 (13.4)	16.8	35.4
New York	$PM_{2.5}$	9.7 (1.6)	8.6	10.9
	PM_{10}	37.7 (18.5)	25.2	48.5
	$PM_{10\text{-}2.5}$	28.4 (19.4)	14.7	39.7
St. Paul	$PM_{2.5}$	8.8 (1.1)	8.0	9.5
	PM_{10}	22.0 (5.6)	17.9	24.5
	$PM_{10\text{-}2.5}$	13.3 (4.8)	9.8	15.4
Winston-Salem	$PM_{2.5}$	12.0 (1.2)	11.4	12.7
	PM_{10}	16.6 (9.7)	12.3	23.4
	$PM_{10\text{-}2.5}$	4.9 (9.3)	0.8	11.4

the intensive sampling data was largely better than these new AOD-models, they were not substantially or consistently so. For example, we previously had CV R^2s of 0.68 (RMSE: 1.16 μg/m^3) and 0.41 (RMSE: 1.09 μg/m^3) in Chicago and Winston Salem, respectively, as compared to CV R^2s of 0.50 (RMSE: 3.48 μg/m^3) and 0.34 (RMSE: 1.79 μg/m^3) for our current models. In contrast, our new St. Paul models have a CV R^2 of 0.85 (RMSE: 3.21 μg/m^3) as compared to our earlier models of 0.51 (RMSE 2.33 μg/m^3). Correspondingly, the correlations between the MESA Coarse measurements and our satellite-based model predictions were moderate to strong in Chicago and St. Paul where our models performed well but poor in Winston-Salem where neither modeling approach performed well. This is reassuring and perhaps not surprising given that the MESA Coarse measurements were taken at specific locations compared to the satellite-based predictions, which have a 1 km^2 spatial resolution. Given that monitoring field studies are very expensive to conduct and cannot easily capture the spatiotemporal variability in $PM_{10\text{-}2.5}$ concentrations, this AOD-informed approach offers important benefits over predictions derived from spatially intensive ground monitoring.

Another study of the whole conterminous US used generalized additive mixed models with geographic, meteorological, and visibility data to predict $PM_{2.5}$ and PM_{10} concentrations at the monthly scale based on EPA monitoring data (Yanosky et al., 2008, 2009, 2014). Over the period from 1999 to 2007 they found a spatial CV R^2 of 0.61 for their $PM_{10\text{-}2.5}$ predictions, with performance that varied across geographical regions from 0.33 in the Southcentral US to 0.64 in the Southwest. Importantly, Yanosky et al. (2014) hypothesized that the inclusion of AOD measures in spatiotemporal models might improve model predictive accuracy, especially in areas distant from air quality monitors. In fact, this did appear to be the case as our final long-term average CV predictions had much better spatial performance in Baltimore, New York, and St. Paul (0.74–0.97 vs. 0.49 to 0.53), better performance in Los Angeles (0.70 vs. 0.64), and marginally better performance in Chicago (0.50 vs. 0.49) than those models. Only in Winston-Salem did their models have better predictive ability, although they also had only modest performance (0.34 vs. 0.36).

Outside of the US, Stafoggia et al. (2019) used AOD measures and a similar approach to ours to predict $PM_{2.5}$, PM_{10}, and $PM_{10\text{-}2.5}$ in Italy, although they first used a Random Forest (RF) design to impute missing AOD values and subsequently used RF rather than mixed models to calibrate PM to AOD. While their predictive performance for $PM_{2.5}$ and PM_{10} was very good, the results for $PM_{10\text{-}2.5}$ were poorer, with the annual spatial CV R^2 ranging from 0.51 to 0.67. $PM_{10\text{-}2.5}$ results were especially poor in summer months and in southern Italy. Interestingly, similar to our findings, Stafoggia et al. (2019) also found better spatial compared to overall and temporal predictive performance for $PM_{10\text{-}2.5}$, whereas $PM_{2.5}$ and PM_{10} performed better overall and temporally.

Differences in our Winston-Salem $PM_{10\text{-}2.5}$ results as compared to those in the Southeast region in Yanosky et al. (2014) highlights one of the key challenges of predicting concentrations for localized areas as we have done in this work. Unlike many other studies that have predicted PM levels across larger regions or nations, our study focused on smaller metropolitan areas. While predicting over smaller areas has the potential to increase accuracy if there is effect modification of predictors by place, it can come at the cost of lost variation in exposures. Notably, there was only a 5 μg/m^3 range in the long-term average $PM_{10\text{-}2.5}$ concentrations in Winston-Salem across the eleven collocated $PM_{10\text{-}2.5}$ sites during our study period. In contrast, our other cities had monitor level averages with ranges closer to 10–20 μg/m^3. This lack of variation surely contributed to our inability to predict the spatial variability in $PM_{10\text{-}2.5}$ levels well.

Fig. 1 and Table 1 highlight a second limitation of studying a smaller area, which is that the models can be informed by relatively few monitoring sites. This limitation likely contributed to the overall poorer results for PM_{10} compared to $PM_{2.5}$ since in all six study areas there were both fewer samplers and measurements for PM_{10} than $PM_{2.5}$. Another

consequence of having fewer monitoring sites when studying a smaller area is that there is often less variation in the types of places where air quality stations are sited. For example, in the New York region all of the PM_{10} monitors were sited in low elevation, urban areas that were near the coast. This resulted in the areas west of the city having many predictor values outside of the design space of the data used to fit the calibration model. This, in combination with the coefficients for these predictors, resulted in high predicted concentrations of PM_{10} (and subsequently $PM_{10\text{-}2.5}$) in the area west of New York City (Fig. 2). A similar phenomenon occurred in Winston-Salem where the PM_{10} stations are all sited in close proximity to the major highways and areas distant to the highways have very low predicted values.

Our models were not fit directly on $PM_{10\text{-}2.5}$ measurements, but rather on $PM_{2.5}$ and PM_{10} separately. In such models, the error from both models contributes to the performance of the predictions. Although this is common for $PM_{10\text{-}2.5}$ modeling due to a lack of size-fraction specific sampling, its impact is highlighted by the strong performance of our $PM_{2.5}$ and PM_{10} models (final model CV R^2 0.93 and 0.77, respectively) in Winston-Salem but not $PM_{10\text{-}2.5}$ (CV R^2 was 0.34). This may be more important in Winston-Salem given that $PM_{10\text{-}2.5}$ levels are largely low and non-variable and that $PM_{2.5}$ is a larger fraction of PM_{10} than in our other areas. Finally, we note that while we performed backward selection with the AIC to select the fixed effects used in each calibration model, future work might explore alternative approaches for dimension reduction and/or regularization in the predictor space. Approaches such as principal component analysis (PCA), partial least squares (PLS), lasso or ridge regression might improve the predictive accuracy of our models by reducing any remaining collinearity.

Overall, however, we had strong performance of our models to characterize the spatial variability of $PM_{10\text{-}2.5}$. In addition, our AOD-based predictions dramatically out-performed the alternative IDW and nearest monitor approaches that have been used in other epidemiology studies to date, showing the potential improvement this approach can offer to environmental epidemiological research. In contrast, the temporal performance of our $PM_{10\text{-}2.5}$ estimates was very poor, with final model mean CV R^2 ranging from 0.15 in Baltimore to 0.42 in Los Angeles, suggesting that this approach does not adequately capture the daily variation in $PM_{10\text{-}2.5}$ concentrations in these six areas. Importantly, though, our poor temporal performance was largely the same as results from the city mean approach (mean temporal R^2 ranged from 0.20 in New York to 0.59 in Los Angeles) that has been frequently deployed in epidemiological studies, raising questions about the impacts of measurement error in the epidemiology on short-term exposures to $PM_{10\text{-}2.5}$ in the United States.

5. Conclusion

In summary, we have demonstrated that the use of satellite AOD data is an effective method for characterizing spatial, but not temporal variations, in $PM_{10\text{-}2.5}$ concentrations in six cities in the US. Notably, our AOD-based predictions had much better performance than alternative IDW and nearest monitor approaches that have been used in many epidemiological research studies of the health impacts of long-term $PM_{10\text{-}2.5}$ exposure. In contrast, our poor temporal performance was largely the same as the alternative city mean approach often used in short term epidemiological research. This demonstrates that $PM_{10\text{-}2.5}$ has more spatiotemporal variability than the current set of EPA monitoring stations can capture, even with the addition of satellite-based information. Given the high costs of field sampling, this AOD-based methodology is a strong option for estimating long-term $PM_{10\text{-}2.5}$ concentrations, especially in areas with sufficient numbers of air quality monitors and spatial variability in concentrations.

CRediT authorship contribution statement

Meredith Pedde: Conceptualization, Methodology, Formal analysis, Data curation, Writing – original draft, Funding acquisition. **Itai Kloog:** Methodology, Writing – review & editing. **Adam Szpiro:** Methodology, Writing – review & editing. **Michael Dorman:** Data curation. **Timothy V. Larson:** Writing – review & editing. **Sara D. Adar:** Conceptualization, Methodology, Writing – review & editing, Supervision, Funding acquisition.

Declaration of competing interest

The authors declare that they have no known competing financial interests or personal relationships that could have appeared to influence the work reported in this paper.

Table A.1
Summary statistics of all daily $PM_{2.5}$, PM_{10}, and $PM_{10\text{-}2.5}$ concentrations ($\mu g/m^3$) measured at EPA air quality monitoring stations in six US metropolitan areas for the period 2000–2012 independent of paired AOD data (i.e., validation dataset)[a].

City	Particle Size	Number of Sites	Number of Observations	Mean	Median	Min	Max	IQR
Baltimore	$PM_{2.5}$	30	39,165	13.2	11.3	0	94.1	9.2
	PM_{10}	13	4694	20.6	18	0	93	13
	$PM_{10\text{-}2.5}$	8	2728	7.8	5.8	−57.1	73.4	7.6
Chicago	$PM_{2.5}$	28	36,159	14.2	12.4	0	68.4	10
	PM_{10}	15	8245	23.3	21	0	110	15
	$PM_{10\text{-}2.5}$	9	4514	9.0	7.3	−18.1	94.0	9.6
Los Angeles	$PM_{2.5}$	22	39,844	16.4	13.6	0	132.6	10.5
	PM_{10}	19	12,928	34.7	32	1	1129	22
	$PM_{10\text{-}2.5}$	12	8294	19.0	16.5	−25.3	491.4	14.1
New York	$PM_{2.5}$	37	44,589	12.5	10.3	0	86.8	9.5
	PM_{10}	11	3011	25.0	21	0	164	17
	$PM_{10\text{-}2.5}$	5	1476	11.0	8.2	−33.4	135.7	10.4
St. Paul	$PM_{2.5}$	17	15,639	10.0	8.4	0	69.9	7
	PM_{10}	8	4639	25.8	23	0	107	16
	$PM_{10\text{-}2.5}$	4	1742	15.6	12.5	−16.9	98.0	12.2
Winston-Salem	$PM_{2.5}$	27	38,321	12.9	11.7	0	99	8.6
	PM_{10}	15	5924	20.3	19	0	99	12
	$PM_{10\text{-}2.5}$	11	3762	6.0	5.5	−22.6	49.4	4.3

[a] These data are, however, restricted to only EPA sites that are used in the calibration model (i.e., sites with >30 observations throughout the study period and only one station per location).

Table A.2
Calibration model coefficients of AIC-selected spatial and temporal predictors (fixed effects), by study area and particle size.

Model Term	Baltimore		Chicago		Los Angeles		New York		St. Paul		Winston-Salem	
	$PM_{2.5}$	PM_{10}	$PM_{2.5}$	PM_{10}	$PM_{2.5}$	PM_{10}	$PM_{2.5}$	PM_{10}	$PM_{2.5}$	PM_{10}	$PM_{2.5}$	PM_{10}
(Intercept)	10.35	17.68	11.99	23.54	14.25	33.57	10.16	24.13	8.05	25.93	10.92	17.98
AOD	7.37	11.64	2.96		18.05	14.67	3.27		4.20		7.23	12.10
avg_elev	−0.14		−0.26	3.51	−1.41	−3.67	−0.21	4.26	0.10			
pct_Open_Water			−0.27									
pct_Dev_Open		3.93	−2.95		4.05	3.44		−2.04				−3.01
pct_Dev_Low	0.64	2.01	−3.55		5.06		0.16					
pct_Dev_Medium	0.36		−4.45		4.85	0.97	0.23		0.40	1.94	0.24	−2.64
pct_Dev_High	0.92	5.31	−2.84	3.01	8.30		0.39		0.26	2.66		
pct_Barren			−1.06									
pct_Decid_Forest	0.42		−2.69	0.82			0.33		0.50	5.22		
pct_EvGrn_Forest											0.10	
pct_Mix_Forest	−0.28										−0.29	
pct_Shrub_Scrub			−0.73									
pct_Grass_Herb				−0.78	1.68	3.45					−0.17	
pct_Pasture_Hay			0.19									
pct_Cultiv_Crop			−0.29									
pct_Woody_Wetland	0.11		−1.03									
pct_Emerg_Herb_Wetland			−0.41									
BG_Population				−9.49		11.82	−2.70	21.87				1.98
BG_Population_Grow		−0.87		12.97		−12.39	3.12	−21.91			−0.13	−2.45
NDVI	0.36	−2.00			0.38	−0.99	−0.31		0.24			
daily_avg_pbl	−1.58	−1.96	−0.52	−1.59	−1.00		−1.43		−0.84		−0.76	−1.03
Evaporation	0.17		−0.62		−0.42		0.52		−1.15			
Humidity	4.18	3.62	2.83	1.49		−8.22	1.57	3.50	2.93			−2.53
PrecipitableWater					−3.47		2.50		−1.30			
Pressure	−0.29				−1.90	−15.61					0.25	1.01
Temperature	−2.59		−1.29		3.41	9.34	−2.37				1.84	4.96
Uwind					0.60		0.73				−0.35	
Visibility	0.39	1.63	−0.24	1.04	0.96	0.92	0.51				0.35	0.97
Vwind	0.82	1.08	1.64	1.68	0.58	1.65	1.14	3.49	1.07	4.19	0.94	1.77
total_roads_km	0.15	2.02	0.34		0.23	2.20			0.27	1.06		
near_prim_rd_m	−0.46		−0.14		−0.36	1.21	−0.26	3.09	−0.16		−0.09	−0.99
near_sec_rd_m	0.19	4.71	0.45	4.71	−0.48		−0.30	−4.56				1.30
near_railroad_m				−2.14			−0.09	−4.17				−1.09
near_water_m				1.95	0.29							
near_big_water_m	−0.13	2.89				−16.08	−0.26	2.41	−0.29		0.37	

Table A.3
Summary statistics [mean(SD)] of meteorological predictors by study area for the period 2000–2012.

City	Planetary Boundary Layer (m)	Evaporation (kg/m2)	Humidity (kg/kg)	Precipitable Water (kg/m2)	Pressure (Pa)	Temperature (K)	U-wind (m/s)	Visibility (m)	V-wind (m/s)
Baltimore	707 (303)	0.32 (0.22)	0.008 (0.005)	22 (12)	100,436 (1035)	286 (10)	1.1 (2.5)	17,643 (3633)	0.0 (2.6)
Chicago	547 (248)	0.30 (0.24)	0.007 (0.005)	19 (11)	99,204 (705)	284 (11)	0.9 (2.9)	17,052 (4326)	0.6 (3.1)
Los Angeles	494 (226)	0.10 (0.08)	0.006 (0.002)	13 (7)	92,010 (4052)	289 (6)	1.1 (1.9)	18,759 (2665)	0.8 (1.9)
New York	691 (292)	0.30 (0.22)	0.008 (0.005)	21 (12)	100,912 (983)	285 (9)	1.4 (3.2)	17,172 (3913)	−0.1 (2.7)
St. Paul	636 (293)	0.27 (0.25)	0.006 (0.004)	16 (11)	98,050 (718)	281 (13)	0.7 (2.6)	16,437 (5070)	0.4 (2.9)
Winston-Salem	663 (290)	0.33 (0.21)	0.009 (0.005)	24 (13)	98,700 (1420)	289 (9)	0.8 (2.4)	18,059 (3358)	0.2 (2.2)

Acknowledgements

Funding: This work was supported by the American Heart Association [Predoctoral Fellowship 17PRE33440000] and the University of Michigan, School of Public Health, Israel Initiative [summer 2016].

References

Adar, S.D., Filigrana, P.A., Clements, N., Peel, J.L., 2014. Ambient coarse particulate matter and human health: a systematic review and meta-analysis. Curr. Environ. Health Rep. 1, 258–274.

Belle, J.H., Chang, H.H., Wang, Y., Hu, X., Lyapustin, A., Liu, Y., 2017. The potential impact of satellite-retrieved cloud parameters on ground-level $PM_{2.5}$ mass and composition. Int. J. Environ. Res. Publ. Health 14, 1244.

Bild, D.E., Bluemke, D.A., Burke, G.L., Detrano, R., Diez Roux, A.V., Folsom, A.R., et al., 2002. Multi-ethnic study of Atherosclerosis: objectives and design. Am. J. Epidemiol. 156, 871–881.
Chen, Y., Yang, Q., Krewski, D., Shi, Y., Burnett, R.T., McGrail, K., 2004. Influence of relatively low level of particulate air pollution on hospitalization for COPD in elderly people. Inhal. Toxicol. 16, 21–25.
Chen, C.H., Chan, C.C., Chen, B.Y., Cheng, T.J., Guo, Y.L., 2015. Effects of particulate air pollution and ozone on lung function in non-asthmatic children. Environ. Res. 137, 40–48.
Christiansen, A.E., Carlton, A.G., Henderson, B.H., 2020. Differences in fine particle chemical composition on clear and cloudy days. Atmos. Chem. Phys. 20, 11607–11624.
Christopher, S.A., Gupta, P., 2010. Satellite remote sensing of particulate matter air quality: the cloud-cover problem. J. Air Waste Manag. Assoc. 60 (5), 596–602.
de Hoogh, K., Héritier, H., Stafoggia, M., Künzli, N., Kloog, I., 2018. Modelling daily PM2.5 concentrations at high spatio-temporal resolution across Switzerland. Environ. Pollut. 233, 1147–1154.
Dee, D.P., Uppala, S.M., Simmons, A.J., Berrisford, P., Poli, P., Kobayashi, S., Andrae, U., Balmaseda, M.A., Balsamo, G., Bauer, P., Bechtold, P., Beljaars, A.C.M., van de Berg, L., Bidlot, J., Bormann, N., Delsol, C., Dragani, R., Fuentes, M., Geer, A.J., Vitart, F., 2011. The ERA-Interim reanalysis: configuration and performance of the data assimilation system. Q. J. R. Meteorol. Soc. 137, 553–597.
Didan, K., 2015. MYD13A3 MODIS/Aqua Vegetation Indices Monthly L3 Global 1km SIN Grid V006. distributed by NASA EOSDIS Land Processes DAAC.
Hu, X., Waller, L.A., Lyapustin, A., Wang, Y., Al-Hamdan, M.Z., Crosson, W.L., Estes Jr., M.G., Estes, S.M., Quattrochi, D.A., Puttaswamy, S.J., Liu, Y., 2014. Estimating ground-level PM2.5 concentrations in the Southeastern United States using MAIAC AOD retrievals and a two-stage model. Remote Sens. Environ. 140, 220–232.
Hu, Z., 2009. Spatial analysis of MODIS aerosol optical depth, PM2.5, and chronic coronary heart disease. Int. J. Health Geogr. 8, 27–36.
Just, A.C., Wright, R.O., Schwartz, J., Coull, B.A., Baccarelli, A.A., Tellez-Rojo, M.M., Moody, E., Wang, Y., Lyapustin, A., Kloog, I., 2015. Using high-resolution satellite aerosol optical depth to estimate daily PM2.5 geographical distribution in Mexico city. Environ. Sci. Technol. 49, 8576–8584.
Kloog, I., Koutrakis, P., Coull, B.A., Lee, H.J., Schwartz, J., 2011. Assessing temporally and spatially resolved PM2.5 exposures for epidemiological studies using satellite aerosol optical depth measurements. Atmos. Environ. 45, 6267–6275.
Kloog, I., Nordio, F., Coull, B.A., Schwartz, J., 2012a. Incorporating local land use regression and satellite aerosol optical depth in a hybrid model of spatiotemporal PM2.5 exposures in the Mid-Atlantic states. Environ. Sci. Technol. 46, 11913–11921.
Kloog, I., Coull, B.A., Zanobetti, A., Koutrakis, P., Schwartz, J.D., 2012b. Acute and chronic effects of particles on hospital admissions in New-England. PLoS One 7, 2–9.
Kloog, I., Chudnovsky, A.A., Just, A.C., Nordio, F., Koutrakis, P., Coull, B.A., Lyapustin, A., Wang, Y., Schwartz, J., 2014. A new hybrid spatio-temporal model for estimating daily multi-year PM2.5 concentrations across northeastern USA using high resolution aerosol optical depth data. Atmos. Environ. 95, 581–590.
Kloog, I., Sorek-Hamer, M., Lyapustin, A., Coull, B., Wang, Y., Just, A.C., Schwartz, J., Broday, D.M., 2015. Estimating daily PM 2.5 and PM 10 across the complex geo-climate region of Israel using MAIAC satellite-based AOD data. Atmos. Environ. 122, 409–416.
Lagudu, U.R.K., Raja, S., Hopke, P.K., Chalupa, D.C., Utell, M.J., Casuccio, G., Lersch, T. L., West, R.R., 2011. Heterogeneity of coarse particles in an urban area. Environ. Sci. Technol. 45, 3288–3296.
Lee, M., Kloog, I., Chudnovsky, A., Lyapustin, A., Wang, Y., Melly, S., Coull, B., Koutrakis, P., Schwartz, J., 2016. Spatiotemporal prediction of fine particulate matter using high-resolution satellite images in the Southeastern US 2003-2011. J. Expo. Sci. Environ. Epidemiol. 26, 377–384.
Levy, R.C., Remer, L.A., Mattoo, S., Vermote, E.F., Kaufman, Y.J., 2007. Second-generation operational algorithm: retrieval of aerosol properties over land from inversion of Moderate Resolution Imaging Spectroradiometer spectral reflectance. J. Geophys. Res. 112, D13211.
Lin, M., Stieb, D.M., Chen, Y., 2005. Coarse particulate matter and hospitalization for respiratory infections in children younger than 15 Years in toronto: a case-crossover analysis. Pediatrics 116, 235–240.
Lipsett, M.J., Tsai, F.C., Roger, L., Woo, M., Ostro, B.D., 2006. Coarse particles and heart rate variability among older adults with coronary artery disease in the coachella valley, claifornia. Environ. Health Perspect. 114, 1215–1220.
Lyapustin, A., Martonchik, J., Wang, Y., Laszlo, I., Korkin, S., 2011a. Multi-angle implementation of atmospheric correction (MAIAC): 1. Radiative transfer basis and look-up tables. J. Geophys. Res. 116, D03210.
Lyapustin, A., Wang, Y., Laszlo, I., Kahn, R., Korkin, S., Remer, L., Levy, R., Reid, J.S., 2011b. MultiAngle implementation of atmospheric correction (MAIAC): 2. Aerosol algorithm. J. Geophys. Res. 116, D03211.
Lyapustin, A.I., Wang, Y., Laszlo, I., Hilker, T., Hall, F.G., Sellers, P.J., Tucker, C.J., Korkin, S.V., 2012. Multi-angle implementation of atmospheric correction for MODIS (MAIAC). 3: atmospheric correction. Remote Sens. Environ. 127, 385–393.
Madrigano, J., Kloog, I., Goldberg, R., Coull, B.A., Mittleman, M.A., Schwartz, J., 2013. Long-term exposure to PM2.5 and incidence of acute myocardial infarction. Environ. Health Perspect. 121, 192–196.
Malig, B.J., Green, S., Basu, R., Broadwin, R., 2013. Coarse particles and respiratory emergency department visits in California. Am. J. Epidemiol. 178, 58–69.
Manson, S., Schroeder, J., Van Riper, D., Ruggles, S., 2018. IPUMS National Historical Geographic Information System: Version 13.0 [Database]. University of Minnesota, Minneapolis.
McGuinn, L.A., Ward-Caviness, C.K., Neas, L.M., Schneider, A., Diaz-Sanchez, D., Cascio, W.E., Kraus, W.E., Hauser, E., Dowdy, E., Haynes, C., Chudnovsky, A., Koutrakis, P., Devlin, R.B., 2016. Association between satellite-based estimates of long-term PM2.5 exposure and coronary artery disease. Environ. Res. 145, 9–17.
Mesinger, F., DiMego, G., Kalnay, E., Mitchell, K., Shafran, P.C., Ebisuzaki, W., Jovic, D., Woollen, J., Rogers, E., Berbery, E.H., Ek, M.B., Fan, Y., Grumbine, R., Higgins, W., Li, H., Lin, Y., Manikin, G., Parrish, D., Shi, W., 2006. North American regional reanalysis. Bull. Am. Meteorol. Soc. 87, 343–360.
Miller, K.A., Siscovick, D.S., Sheppard, L., Shepherd, K., Sullivan, J.H., Anderson, G.L., Kaufman, J.D., 2007. Long-term exposure to air pollution and incidence of cardiovascular events in women. N. Engl. J. Med. 356, 447–458.
Nordio, F., Kloog, I., Coull, B.A., Chudnovsky, A., Grillo, P., Bertazzi, P.A., Baccarelli, A. A., Schwartz, J., 2013. Estimating spatio-temporal resolved PM10 aerosol mass concentrations using MODIS satellite data and land use regression over Lombardy, Italy. Atmos. Environ. 74, 227–236.
Pakbin, P., Hudda, N., Cheung, K.L., Moore, K.F., Sioutas, C., 2010. Spatial and temporal variability of coarse (PM10-2.5) particulate matter concentrations in the Los Angeles area. Aerosol Sci. Technol. 44, 514–525.
Peng, R.D., Chang, H.H., Bell, M.L., McDermott, A., Zeger, S.L., Samet, J.M., Dominici, F., 2008. Coarse particulate matter air pollution and hospital admissions for cardiovascular and respiratory diseases among medicare patients. JAMA 299, 2172–2179.
R Core Team, 2018. R: A Language and Environment for Statistical Computing. R Foundation for Statistical Computing, Vienna, Austria.
R Core Team, 2019. R: A Language and Environment for Statistical Computing. R Foundation for Statistical Computing, Vienna, Austria.
Remer, L.A., Kaufman, Y.J., Tanré, D., Mattoo, S., Chu, D.A., Martins, J.V., Li, R.R., Ichoku, C., Levy, R.C., Kleidman, R.G., Eck, T.F., Vermote, E., Holben, B.N., 2005. The MODIS aerosol algorithm, products, and validation. J. Atmos. Sci. 62, 947–973.
Rodopoulou, S., Chalbot, M.C., Samoli, E., Dubois, D.W., San Filippo, B.D., Kavouras, I. G., 2014. Air pollution and hospital emergency room and admissions for cardiovascular and respiratory diseases in Doña Ana County, New Mexico. Environ. Res. 129, 39–46.
Sawvel, E.J., Willis, R., West, R.R., Casuccio, G.S., Norris, G., Kumar, N., Hammond, D., Peters, T.M., 2015. Passive sampling to capture the spatial variability of coarse particles by composition in Cleveland, OH. Atmos. Environ. 105, 61–69.
Shtein, A., Karnieli, A., Katra, I., Raz, R., Levy, I., Lyapustin, A., Dorman, M., Broday, D. M., Kloog, I., 2018. Estimating daily and intra-daily PM10 and PM2.5 in Israel using a spatio-temporal hybrid modeling approach. Atmos. Environ. 191, 142–152.
Sorek-Hamer, M., Just, A.C., Kloog, I., 2016. Satellite remote sensing in epidemiological studies. Curr. Opin. Pediatr. 28, 228–234.
Stafoggia, M., Samoli, E., Alessandrini, E., Cadum, E., Ostro, B., Berti, G., Faustini, A., Jacquemin, B., Linares, C., Pascal, M., Randi, G., Ranzi, A., Stivanello, E., Forastiere, F., MED-PARTICLES Study Group, 2013. Short-term associations between fine and coarse particulate matter and hospitalizations in Southern Europe: results from the MED-PARTICLES project. Environ. Health Perspect. 121, 1026–1033.
Stafoggia, M., Schwartz, J., Badaloni, C., Bellander, T., Alessandrini, E., Cattani, G., de' Donato, F., Gaeta, A., Leone, G., Lyapustin, A., Sorek-Hamer, M., de Hoogh, K., Di, Q., Forastiere, F., Kloog, I., 2017. Estimation of daily PM10 concentrations in Italy (2006-2012) using finely resolved satellite data, land use variables and meteorology. Environ. Int. 99, 234–244.
Stafoggia, M., Bellander, T., Bucci, S., Davoli, M., de Hoogh, K., de' Donato, F., Gariazzo, C., Lyapustin, A., Michelozzi, P., Renzi, M., Scortichini, M., Shtein, A., Viegi, G., Kloog, I., Schwartz, J., 2019. Estimation of daily PM10 and PM2.5 concentrations in Italy, 2013-2015, using a spatiotemporal land-use random-forest model. Environ. Int. 124, 170–179.
Thornburg, J., Rodes, C.E., Lawless, P.A., Williams, R., 2009. Spatial and temporal variability of outdoor coarse particulate matter mass concentrations measured with a new coarse particle sampler during the Detroit Exposure and Aerosol Research Study. Atmos. Environ. 43, 4251–4258.
US Census Bureau, 2012. 2010 TIGER/Line Shapefiles [machine-Readable Data Files]/ Prepared by the U.S. Census Bureau.
US EPA, 2019. Integrated Science Assessment (ISA) for Particulate Matter (Final Report, Dec 2019). U.S. Environmental Protection Agency, Washington, DC. EPA/600/R-19/188.
US EPA, 2009. Integrated Science Assessment (ISA) for Particulate Matter (Final Report, Dec 2009). U.S. Environmental Protection Agency, Washington, DC. EPA/600/R-08/139F.
USGS, 2001. NLCD 2001 Land Cover Conterminous United States Remote-Sensing Image: Sioux Falls. SD, USGS.
USGS, 2006. NLCD 2006 Land Cover Conterminous United States Remote-Sensing Image: Sioux Falls. SD, USGS.
USGS, 2011. NLCD 2011 Land Cover Conterminous United States Remote-Sensing Image: Sioux Falls. SD, USGS.
USGS, 2017. 1/3rd Arc-Second Digital Elevation Models (DEMs) - USGS National Map 3DEP Downloadable Data Collection: U.S. Geological Survey.
USGS, 2019. National Hydrography Dataset (Ver. USGS National Hydrography Dataset Best Resolution (NHD) for Hydrologic Unit (HU) 4 - 2001 (published 20191002)).
Wilson, W.E., Suh, H.H., 1997. Fine particles and coarse particles: concentration relationships relevant to epidemiologic studies. J. Air Waste Manag. Assoc. 47, 1238–1249.
Yanosky, J.D., Paciorek, C.J., Schwartz, J., Laden, F., Puett, R., Suh, H.H., 2008. Spatio-temporal modeling of chronic PM10 exposure for the nurses' health study. Atmos. Environ. 42, 4047–4062.

Yanosky, J.D., Paciorek, C.J., Suh, H.H., 2009. Predicting chronic fine and coarse particulate exposures using spatiotemporal models for the northeastern and midwestern United States. Environ. Health Perspect. 117, 522–529.
Yanosky, J.D., Paciorek, C.J., Laden, F., Hart, J.E., Puett, R.C., Liao, D., Suh, H.H., 2014. Spatio-temporal modeling of particulate air pollution in the conterminous United States using geographic and meteorological predictors. Environ. Health 13, 63–77.
Zhang, K., Larson, T.V., Gassett, A., Szpiro, A.A., Daviglus, M., Burke, G.L., Kaufman, J. D., Adar, S.D., 2014. Characterizing spatial patterns of airborne coarse particulate (PM10-2.5) mass and chemical components in three cities: the multi-ethnic study of Atherosclerosis. Environ. Health Perspect. 122, 823–830.
Zhao, Y., Wang, S., Lang, L., Huang, C., Ma, W., Lin, H., 2017. Ambient fine and coarse particulate matter pollution and respiratory morbidity in Dongguan, China. Environ. Pollut. 222, 126–131.